Northern Hemispheric Storm tracks in the NOAA/NCEP GFS and CFS Models: Climatology, Interannual Variability, and Extreme Events.

Timothy Eichler and R. Wayne Higgins
Climate Prediction Center / NCEP

1. Introduction

Software designed to generate stormtracks was applied to SLP data (both four times and 2 times daily) from the GFS and CFS models. The GFS model is an atmospheric general circulation model (AGCM) with a T62 resolution which was run from 1950-2002 using AMIP SSTs as a bottom boundary condition. The CFS is a fully coupled model consisting of the GFS atmospheric model coupled to the GFDL MOM III ocean model. The CFS simulation was a climatological free run which was run from 2002-2033.

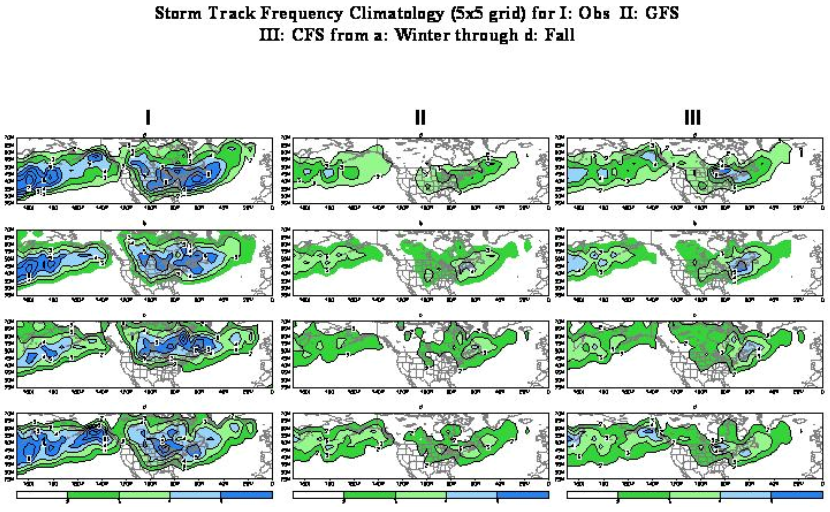

Figure 1

2. Stormtrack Climatology

Stormtrack frequency seasonal climatologies were tabulated by binning the storms into 5x5 gridboxes and averaging for specific seasons over all times (e.g. JFM frequency climatology was generated by averaging over all JFM periods). Figure 1 shows the stormtrack frequency for observations as well as the GFS and CFS models. Note the preferred stormtracks across the North Pacific, the Great Lakes, and along the U.S. east coast. Also note that the GFS and CFS models produce fewer storms than observed.

Figure 2 shows where the GFS and CFS underestimate observed stormtrack frequency for JFM. In both the GFS and CFS models (Fig. 2a and 2b respectively), there is a marked decrease in stormtrack frequency especially east of Japan, the

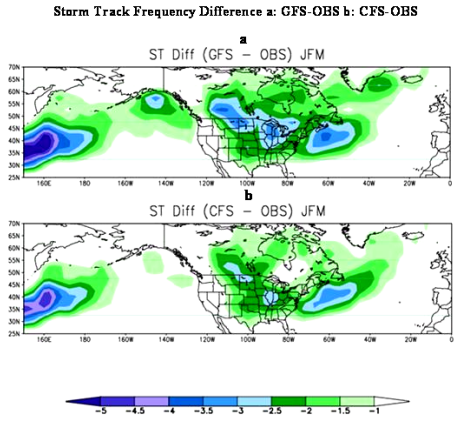

Figure 2

Great Lakes, and just off the U.S. east coast.

Differencing the CFS and GFS model stormtrack frequency shows that the CFS tends to do better than the GFS model (although not as good as observed) east of Japan, the northeastern Pacific, and in the Great lakes region (fig. 3).

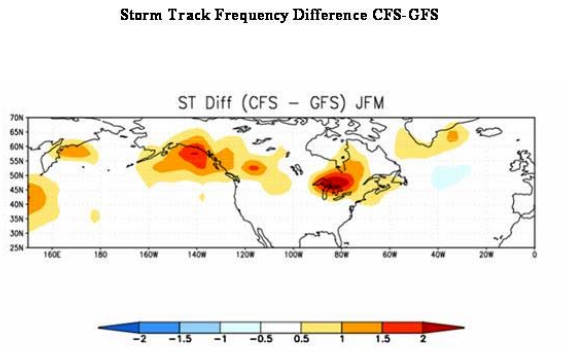

Figure 3

As would be expected, the GFS and CFS have reduced variability compared to observations (Fig. 4). In both the GFS and CFS models, the highest variability of SLP occurs over the "centres of action" associated with the Aleutian and Icelandic lows (I: fig. 4a and II: fig. 4a respectively). A similar pattern is shown for the observed data (Fig. 4b). A difference between the GFS and CFS models and observations (Figs. 4c I and II) shows that the models have less variability of SLP at high latitudes, the Aleutians, and Iceland and increased variability from East Africa to Korea. The areas of decreased variability in the Aleutian Islands and Iceland correspond well to areas of decreased storm frequency seen in the models. The area of increased variability seen over Asia needs to be studied further to determine the cause (e.g. model topography).

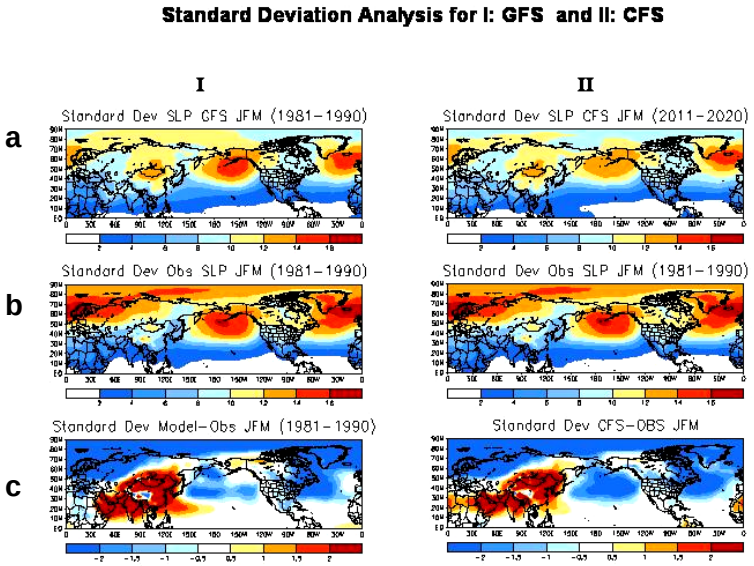

Figure 4

Interannual Variability

To assess how stormtracks change as a function of ENSO phase, stormtracks were composited for strong El Nino, weak El Nino, neutral, weak La Nina and strong La Nina. To accomplish this, the EIS, which is a four-class intensity scale calculated by doubling the Oceanic Niño Index (ONI), defined as the three-month running mean of SST anomalies for the NINO 3.4 region was used. The observed stormtracks as a function of El Nino are shown in Figure 5. Note that for strong El Nino (Fig. 5a) well defined stormtracks are seen across the north Pacific, the Great Lakes and from the southeastern U.S. northeastward to east of Greenland. As one proceeds from strong El Nino

to strong La Nina (from fig. 5a to 5e), the north Pacific and north Atlantic stormtracks shift northward and the Great Lakes stormtrack becomes better defined.

Storm Tracks by El Nino Phase (OBS) a: Strong El Nino b: Weak El Nino c: Neutral d: weak La Nina e: Strong La Nina.

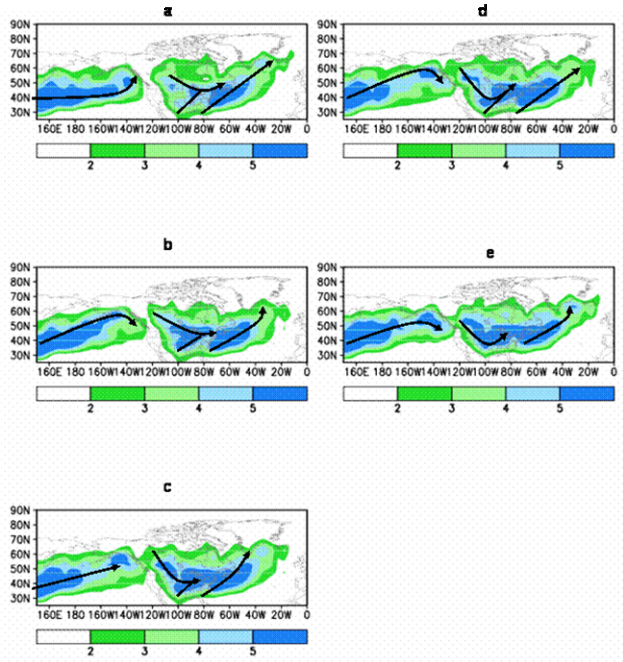

Figure 5

While a similar response to El Nino is noted for the GFS and CFS models, the stormtrack frequency pattern is weaker than observed (Figs. 6 and 7 for GFS and CFS, respectively).

Storm Tracks by El Nino Phase (GFS Model) a: Strong El Nino b: Weak El Nino c: Neutral d: weak La Nina e: Strong La Nina.

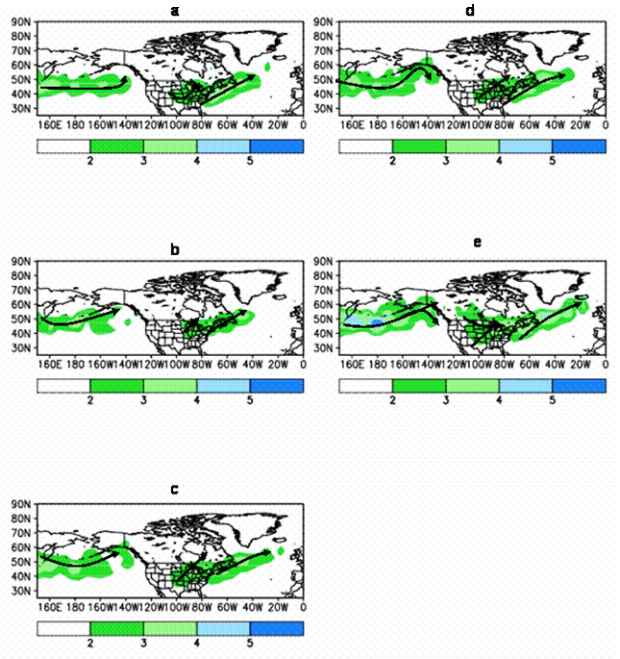

Figure 6

Storm Tracks by El Nino Phase (CFS Model) a: Strong El Nino b: Weak El Nino c: Neutral d: weak La Nina e: Strong La Nina.

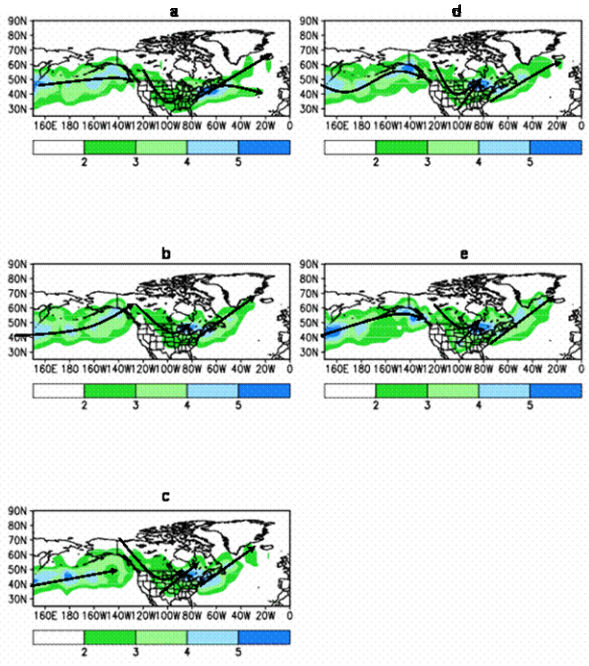

Figure 7

To analyze the changes in stormtracks during strong El Nino and strong La Nina, frequency differences were computed between strong El Nino (la Nina) and neutral conditions. For observed stormtracks (Fig. 8), an increase in storms is seen over the north-central Pacific and along the U.S. east coast with a decrease in frequency across much of the northern half of the U.S. and Canada during El Nino(fig. 8a). For La Nina, the pattern is reversed with decreases across the north-central Pacific and the southern U.S/central North Atlantic and increases from the far northern Pacific eastward to southern Greenland (Fig. 8b).

Composite Stormtrack Frequency Anomaly for a: Strong El Nino-neutral and b: strong La Nina-neutral

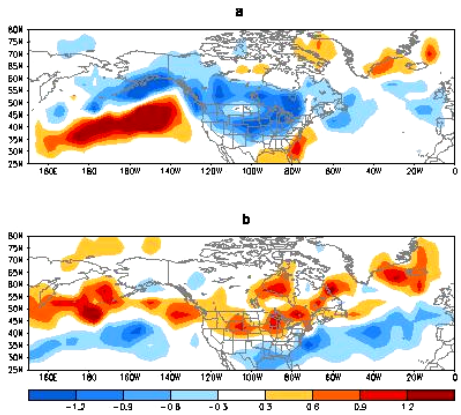

Figure 8

The GFS model shows a similar response to ENSO phase as observed (Fig. 9). An increase in storms during El Nino is seen in the north-central Pacific (though weaker than observed) while the increased storminess along the east coast compares well with observed (Fig. 9a); a general decrease in storms is seen across the far northern Pacific, southern Canada, and the northern half of the U.S. similar to observed (fig. 9a). During La Nina, increases in storms across the far northern Pacific, Canada, the northern U.S., and the North Atlantic agree well with observations (fig. 9b); however, the decrease in storms seen across the central Pacific, southern U.S., and central north Atlantic for observations is not seen in the GFS model (compare fig. 9b with 8b).

Composite GFS Stormtrack Frequency Anomaly for a: Strong El Nino-Neutral and b: Strong La Nina-Neutral

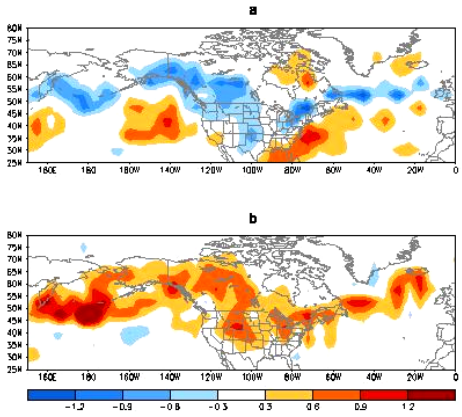

Figure 9

The CFS model shows an interesting asymmetric pattern during El Nino with a noisy pattern across the north Pacific (unlike observations) and a well defined increase (decrease) in storms along the east coast (southern Canada) (Fig.10a). For La Nina, an increase (decrease) in storms associated with the Great Lakes (east coast) stormtracks is seen although the pattern is somewhat less-defined than observed.

Composite CFS Stormtrack Frequency Anomaly for a: Strong El Nino-Neutral and b: Strong La Nina-Neutral

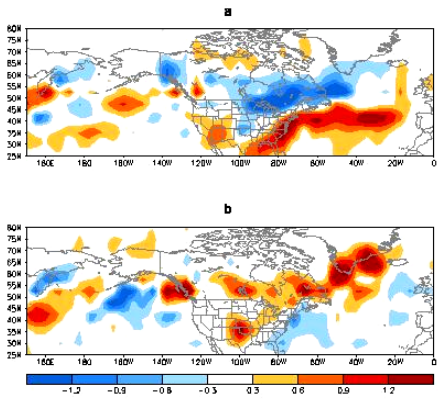

Figure 10

Merdional Temp. Gradient ((degrees C/ km)*100) for a: obs b: GFS model c: GFS-obs

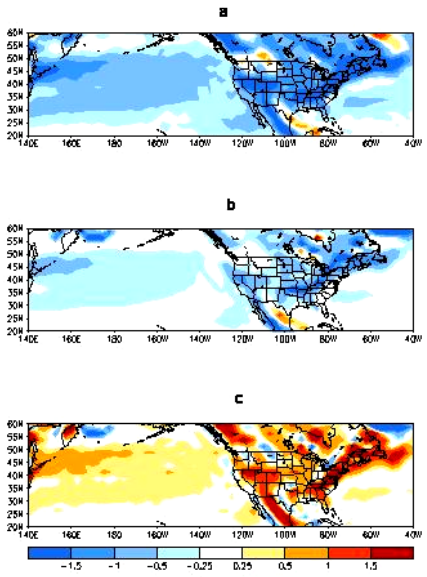

Figure 11

Merdional Temp. Gradient ((degrees C/ km)*100) for a: obs b: CFS model c: CFS-obs

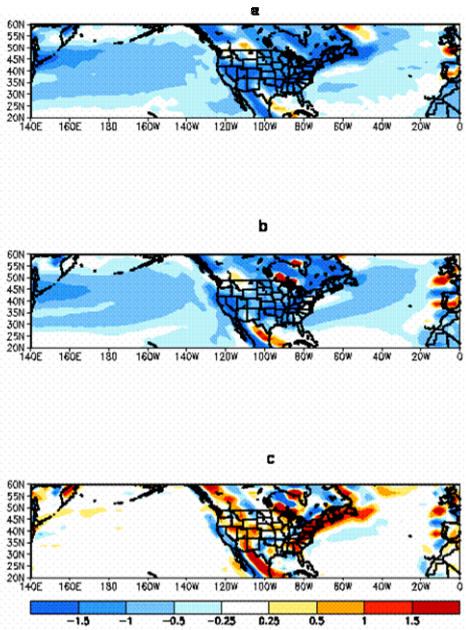

Figure 12

Model Physics/conclusions

The message the models are giving regarding stormtracks is that they (i.e. the GFS and CFS models) capture the general features of observed stormtracks but are less frequent than observed. The simple explanation is that the model SLP fields are less variable. The question is why? One possible reason is that the models have weaker meridional temperature gradients than observed. Figure 11 shows the meridional temperature gradient for JFM. The observed gradient (Fig. 11a) shows a general decrease in temperatures with latitude as expected. Although the GFS model has a similar pattern (Fig. 11b), the overall gradient is weaker than observed (Fig. 11c). For the CFS model, the pattern is less consistent although the temperature gradient is less along the east coast (Fig. 12).

Although the GFS and CFS models generally show less baroclinicity than observations, the pattern is not sufficiently strong to suggest decreased baroclinicity as a reason for decreased storm frequency. It is probable that that the overall variability of SLP is less than observed (rather than just low pressure systems). To verify this hypothesis, the stormtracks program is analyzing the frequency of high pressure systems in observed and model data.